Optics and Laser Technology 126 (2020) 106084

Contents lists available at ScienceDirect

Optics and Laser Technology

journal homepage: www.elsevier.com/locate/optlastec

Passively Q-switched Tm:$YAlO_3$ laser based on WS_2/MoS_2 two-dimensional nanosheets at 2 μm

Yufei Ma[a,*], Haiyue Sun[a], Baofa Ran[a], Shanchun Zhang[a], Han Zhang[b], Frank K. Tittel[c], Zhiwei Lv[d]

[a] National Key Laboratory of Science and Technology on Tunable Laser, Harbin Institute of Technology, Harbin 150001, China
[b] Shenzhen Engineering Laboratory of Phosphorene and Optoelectronics, Collaborative Innovation Center for Optoelectronic Science and Technology, and Key Laboratory of Optoelectronic Devices and Systems of Ministry of Education and Guangdong Province, Shenzhen University, Shenzhen 518060, China
[c] Department of Electrical and Computer Engineering, Rice University, 6100 Main Street, Houston, TX 77005, USA
[d] School of Electronic and Information Engineering, Hebei University of Technology, Tianjin 300401, China

HIGHLIGHTS

- WS_2 and MoS_2 nanosheets were synthesized by CVD method.
- The microstructure and optical characteristics of the nanosheets were investigated.
- Tm:YAP/WS_2 and Tm:YAP/MoS_2 laser performance was compared.

ABSTRACT

A comparison of the pulsed laser performances of 2 μm passively Q-switched Tm:$YAlO_3$ (YAP) lasers based on the use of tungsten disulfide (WS_2) and molybdenum disulfide (MoS_2) two-dimensional (2D) nanosheets as saturable absorbers is reported. The novel nanosheets were prepared by chemical vapor deposition (CVD) technology. The microstructure and optical characteristics of the nanosheets were investigated experimentally. In a continuous-wave (CW) operation, the maximum output power of 2.8 W was obtained at an absorbed pump power of 6.9 W, with a corresponding slope efficiency of 46.4%. In a passively Q-switched operation at a pump power of 1.45 W, the average output power, pulse width, repetition rate, pulse energy, and peak power for the Tm:YAP/WS_2 laser were 0.11 W, 2.65 μs, 34.7 kHz, 2.9 μJ, and 1.23 W, respectively. As for the Tm:YAP/MoS_2 laser, the corresponding values were 0.10 W, 2.5 μs, 24.0 kHz, 3.8 μJ, and 1.55 W.

1. Introduction

Pulsed lasers in the 2 μm region with the advantages of eye-safety and a strong absorption of gas molecules have been widely used in laser processing, environmental monitoring, gas sensing and medical fields [1–3]. Because of its low-cost, easy operation, and compact structure, passively Q-switched technology has been used to generate pulsed lasers [4–6]. Nowadays, ion-doped crystal and graphene serve as saturable absorbers (SAs) in the Q-switched method. However, a narrow operational wavelength and inherent defects are fundamental problems of ion-doped crystals [7]. As for graphene, its low absorption efficiency at 2 μm limits its applications [8].

Semiconducting transition metal dichalcogenides (STMDs) have been developed in recent years. Due to their broad operational bandwidth and short recovery time, tungsten disulfide (WS_2) and molybdenum disulfide (MoS_2) are widely used in near-infrared lasers [9–12]. As two-dimensional (2D) materials in the class of STMDs, WS_2 and MoS_2 have a similar sandwich structure. Their modulation depth can be improved by decreasing the number of layers. The operational wavelength with a few layers can vary from 400 to 2500 nm, corresponding to a direct bandgap [13–16]. The forbidden bandwidth with different numbers of layers is in the range of 1.1–2.1 eV and the maximum forbidden bandwidth of monolayered WS_2 and MoS_2 is 2.1 and 1.9 eV, respectively [17–19]. The thermal conductivity of WS_2 and MoS_2 is 2.2 and 1.05 W/m·K, respectively, which favors thermal diffusion in the Q-switched technique [20]. A 2D nanosheet of STMDs with excellent optical properties has broad application prospects in the mid-infrared spectral region. Therefore, it is meaningful to investigate the mid-infrared pulsed laser properties when WS_2 and MoS_2 are used.

Because of the natural birefringence, $YAlO_3$ (YAP) with a cubic structure is attractive as a laser host. The transition ($^3F_4 \rightarrow {}^3H_6$) of Tm^{3+} is widely used to generate a 2 μm wavelength range laser [21]. YAP has similar mechanical and thermal properties to the classical $Y_3Al_5O_{12}$ (YAG) crystal [22]. However, Tm:YAP has a much larger emission cross section (5.5×10^{-21} cm^{-2}) than that of Tm:YAG (2.2×10^{-21} cm^{-2}) [23,24]. Therefore, the benefit of Tm:YAP is that it

* Corresponding author.
E-mail addresses: mayufei@hit.edu.cn (Y. Ma), hzhang@szu.edu.cn (H. Zhang), zhiweilv@hebut.edu.cn (Z. Lv).

https://doi.org/10.1016/j.optlastec.2020.106084
Received 14 October 2019; Received in revised form 16 January 2020; Accepted 17 January 2020

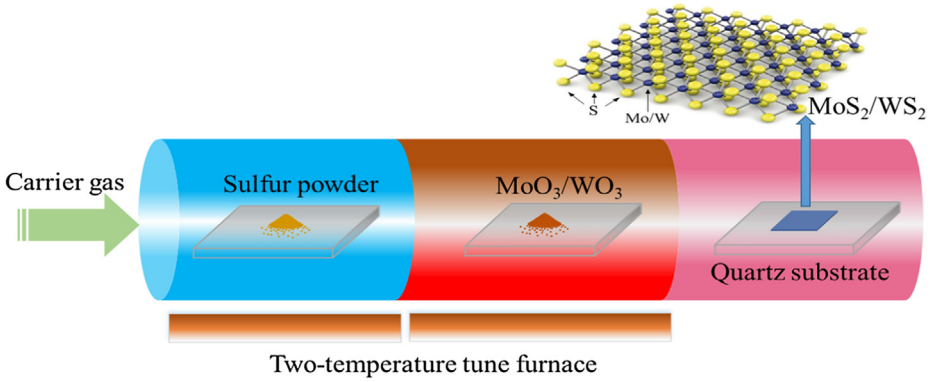

Fig. 1. Schematic representation of the preparation of WS_2 and MoS_2 nanosheets.

can be used to generate 2 μm continuous-wave (CW) and pulsed lasers efficiently. However, there are few reports on WS_2 and MoS_2 passively Q-switched Tm:YAP lasers.

In this paper, a diode-pumped passively Q-switched Tm:YAP at 2 μm with 2D WS_2 and MoS_2 nanosheets was demonstrated for the first time. The WS_2 and MoS_2 nanosheets were prepared by the chemical vapor deposition (CVD) method. The microstructure and optical characteristics of these nanosheets were investigated. The CW and pulsed laser performance were researched respectively.

2. Preparation of WS_2 and MoS_2

WS_2 and MoS_2 nanosheets were successfully prepared by the chemical vapor deposition (CVD) method in this research. As shown in Fig. 1, the high-purity raw materials of MoS_2 were MoO_3 and sulfur powder, which were placed in a two-temperature tube furnace with a diameter of 80 mm. The MoO_3 powder was heated to 650 °C, while the sulfur was heated to 190 °C. For the carrier gas (Ar), they reacted to form MoS_2 in 10 min. The distance between the target quartz substrate and MoO_3 was 5 cm. Similarly, employing Ar and H_2 as a carrier gas, WO_3 (1000 °C) and sulfur (180 °C) reacted in a tube furnace with a diameter of 100 mm to form WS_2 in 20 min. The distance between the target quartz substrate and WO_3 was 1.5 cm.

The Raman spectrometer provided by Renishaw, Inc. was used to measure the Raman spectra of WS_2 and MoS_2. The excitation source of a 532 nm laser was used to avoid the multi-phonon mode. As shown in Fig. 2, the Raman characteristic peaks of A_{1g} and $E_{2g}{}^1$ represent a vibration along and perpendicular to the layers, respectively. The peaks of A_{1g} and $E_{2g}{}^1$ appeared at 353.0 and 419.9 cm^{-1} in the WS_2 nanosheet, respectively. As for the MoS_2 nanosheet, they occurred at 384.9 and 408.8 cm^{-1}, respectively.

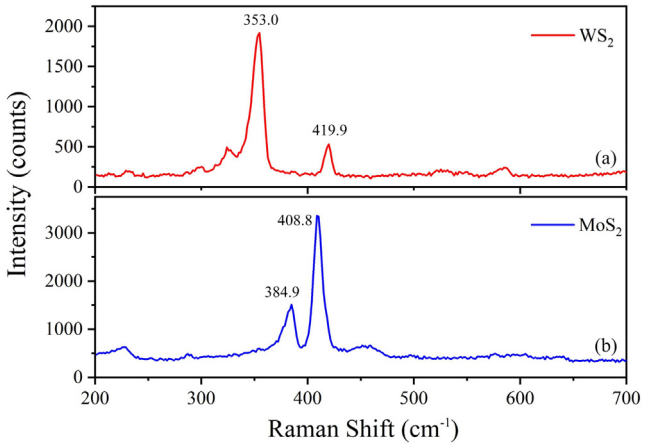

Fig. 2. Raman spectra of (a) WS_2 and (b) MoS_2 from 200 to 700 cm^{-1}.

The number of layers related to the thickness has an influence on the optical and thermal properties of STMDs. An atomic force microscope (AFM) was used to accurately measure the thickness of WS_2 and MoS_2 2D nanosheets in the semi-contact mode. The morphology images and thickness distribution are shown in Fig. 3 and Fig. 4 for WS_2 and MoS_2 2D nanosheets, respectively. The thickness of WS_2 was ~4.5 nm and the number of layers was determined to be 4–5. The thickness of MoS_2 was ~3.2 nm and the number of layers was determined to be 3–4. A spectrophotometer (Solidspec-3700 UV–VIS-NIR, Shimadzu Co., Japan) was used to measure the spectral transmissions of WS_2 and MoS_2 from 1000 to 2000 nm. As shown in Fig. 5, the initial transmission of each SA increased with the measured wavelength. At 1937 nm (the emission peak of the Tm:YAP), the initial total spectral transmissions of WS_2 and MoS_2 were 85.5% and 84.7%, respectively.

The nonlinear total transmissions with different intensities of light were investigated. The light source was a pulsed Tm:YAP laser. The experiment results were fitted using the following formula:

$$T = 1 - q \times \exp(-I/I_{sat}) - \delta_{ns} \quad (1)$$

where T is the transmission, q is the modulation depth, I is the intensity of the laser, I_{sat} is the saturation power intensity, and δ_{ns} is the non-saturable loss. As shown in Fig. 6, the calculated modulation depths of WS_2 and MoS_2 were 8.96% and 13.0%, respectively. The corresponding saturation power intensities were 57.1 and 61.6 MW/cm^2, respectively. The non-saturable losses of WS_2 and MoS_2 were 8.9% and 13.0%, which means that the final saturable transmissions were 91.1% and 87%, respectively.

3. Experimental setup

The experimental setup of the passively Q-switched Tm:YAP laser is shown in Fig. 7. The pump source was a fiber-coupled diode laser operating at 795 nm with a core diameter (φ_0) of 200 μm. The numerical aperture (NA) of the coupled fiber was 0.22. The pump light was focused by the collimating (L1) and focusing (L2) lenses. The focal lengths of L1 and L2 were 26.7 and 42.5 mm, respectively. The magnification factor (κ_m) of the coupling optics was calculated to be 1:1.59. Therefore, the diameter of the focusing spot (d_0) was calculated to be 318 μm by the equation $d_0 = \varphi_0 \times \kappa_m$. A b-cut Tm:YAP crystal with the dimensions of 3 × 3 × 5 mm^3 was used as the active crystal. The Tm^{3+} doping concentration was 3.0 at-%. The temperature of the crystal was set to 20 °C by a water cooling system. WS_2 and MoS_2 nanosheets with a few layers were used as saturable absorbers, respectively. The input plane mirror M1 was coated with an antireflection film at 795 nm and high-reflection film at 2 μm. The output concave lens M2 with a transmission of 5% at 1937 μm had different curvature radii. The length of the laser resonator was 40 mm.

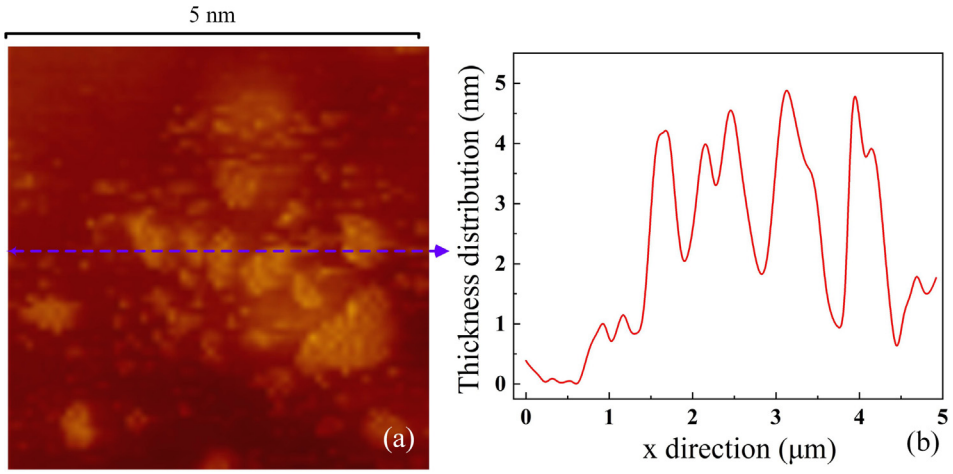

Fig. 3. AFM results of WS_2. (a) morphology image (b) thickness distribution in x the direction (the purple arrow). (For interpretation of the references to color in this figure legend, the reader is referred to the web version of this article.)

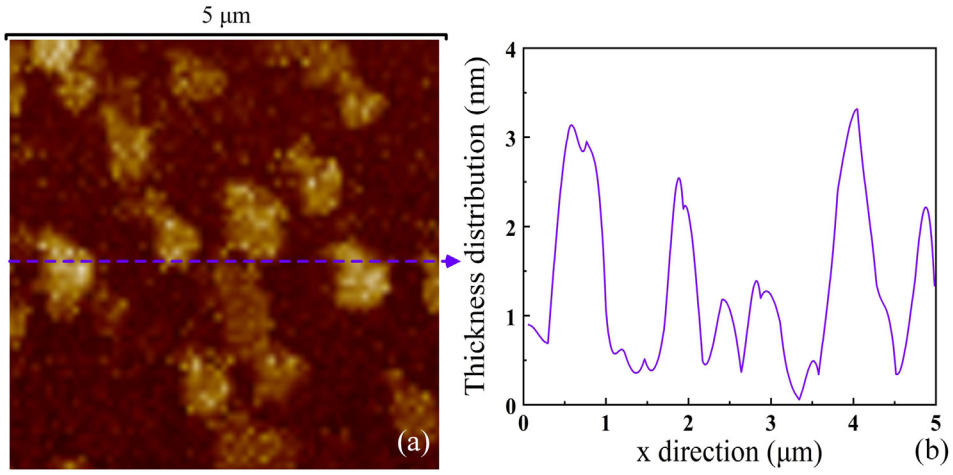

Fig. 4. Atomic force microscope (AFM) results of MoS_2. (a) Morphology image; (b) thickness distribution in the x direction (the purple arrow). (For interpretation of the references to color in this figure legend, the reader is referred to the web version of this article.)

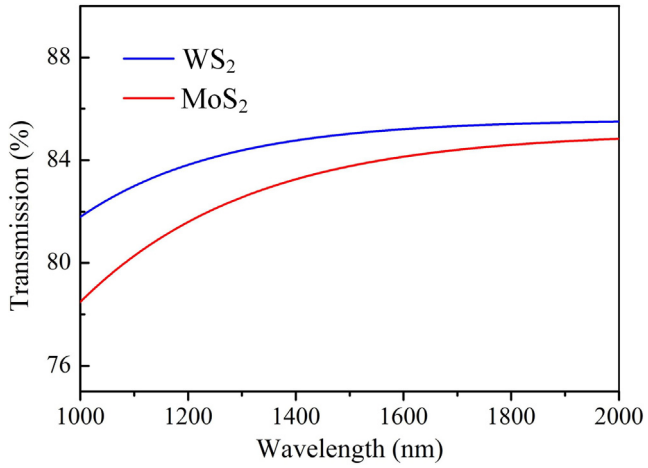

Fig. 5. The total spectral transmissions of WS_2 and MoS_2 from 1000 to 2000 nm.

4. Results and discussion

The relationship between the CW output power and the absorbed pump power was measured first and is shown in Fig. 8. The output concave mirrors with curvature radii (R) of 50, 100, and 200 mm were utilized, respectively. The maximum output power of 2.8 W was obtained at the absorbed pump power of 6.9 W with an R of 50 mm. The corresponding slope efficiency (η_s) and standard error (σ_e) were 46.4% and 0.85%, respectively. The high slope efficiency benefited from the stable cavity and the better mode matching between the pumping laser and the oscillation laser. When the absorbed pump power was 6.9 W, the M2 factors were measured to be 2.4 and 3.2 by the knife-edge method in the parallel and vertical directions, respectively.

As shown in Fig. 9, when the R was 50 mm, the average output power of the passively Q-switched Tm:YAP laser with a WS_2 nanosheet was 0.11 W at an absorbed pump power of 1.45 W. The corresponding slope was 23.8%. As for the Tm:YAP/MoS_2 laser, the average output power and the corresponding slope were 0.10 W and 22.4%, respectively, for the same condition. Compared with the CW situation, a lower absorbed pump power and an average output power were adopted in order to protect WS_2 and MoS_2 saturable absorbers from damage. In addition, the insertion loss of the saturable absorbers had an influence on the average output power. The laser spectrum was measured by a spectrophotometer and is shown in Fig. 10. Compared with the CW laser, the output spectral width was compressed and a blue shift occurred in the passively Q-switched laser with WS_2 and MoS_2 nanosheets.

The pulsed laser performances (pulse width and repetition rate) were measured by a high-speed InGaAs-detector and a digital

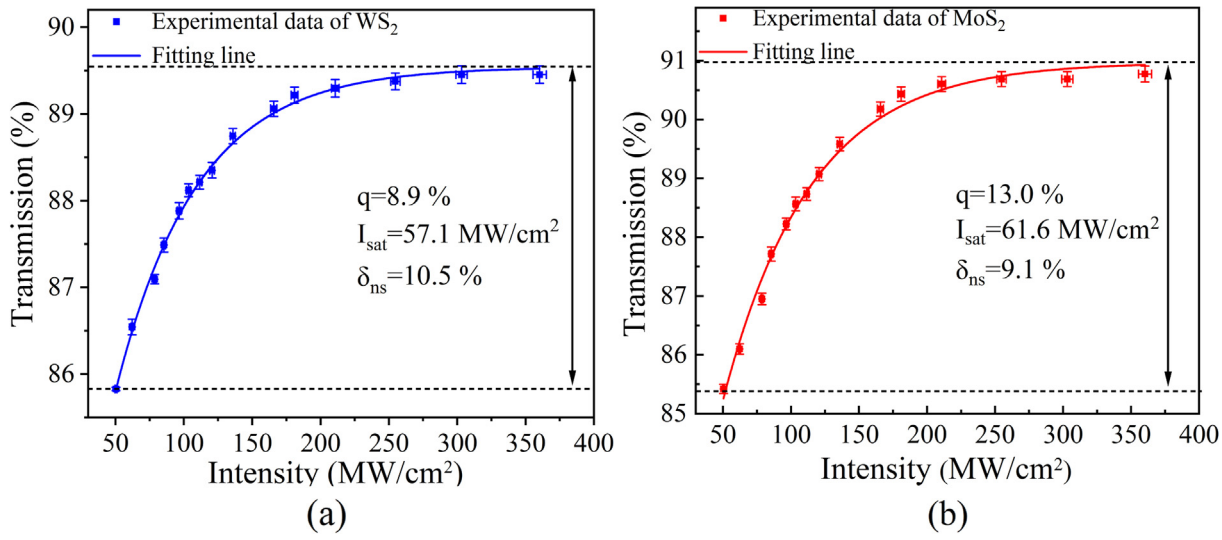

Fig. 6. The nonlinear total transmission of STMDs at 2 μm. (a) WS_2 and (b) MoS_2.

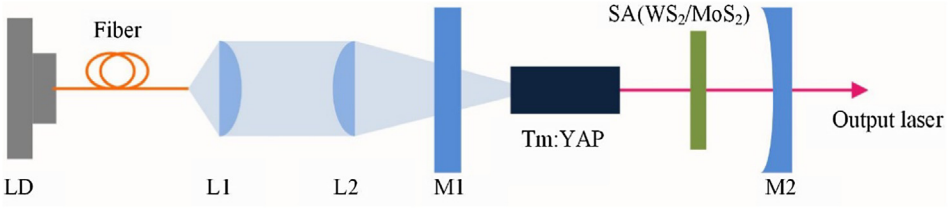

Fig. 7. An experimental schematic diagram of the passively Q-switched Tm:YAP lasers.

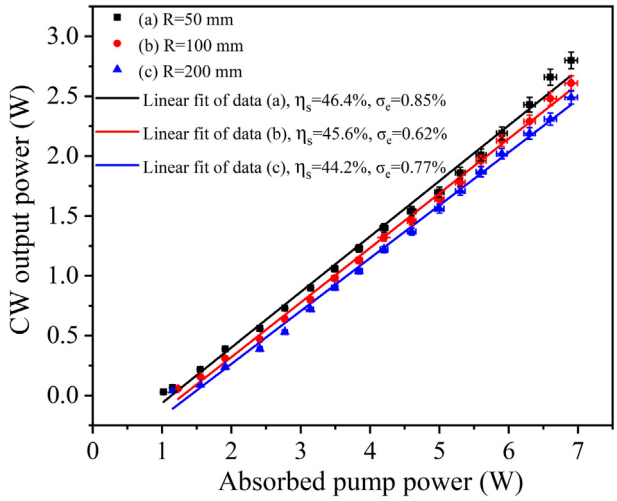

Fig. 8. The relationship between CW output power and absorbed pump power.

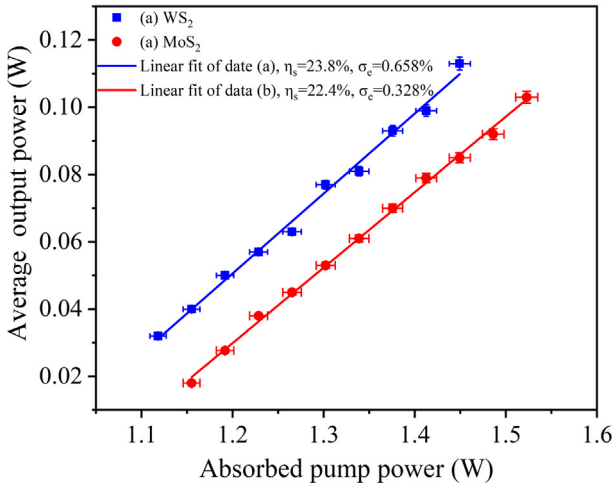

Fig. 9. The relationship between average output power and absorbed pump power.

oscillograph. As shown in Fig. 11(a), at an absorbed pump power of 1.45 W, the obtained pulse widths for Tm:YAP/WS_2 and Tm:YAP/MoS_2 lasers were 2.65 and 2.50 μs, respectively. The narrower minimum pulse width for the 2D MoS_2 nanosheet resulted from the fewer layers and the larger modulation depth. As shown in Fig. 11(b), contrary to the pulse width, the repetition rate increased with the absorbed pump power. The obtained maximum repetition rates for Tm:YAP/WS_2 and Tm:YAP/MoS_2 lasers were 34.7 and 24.0 kHz, respectively. The jitter of the pulse width and the repetition rate of the Q-switched lasers were monitored to be less than 5% for ten minutes. The pulse energy and the peak power were calculated and are shown in Fig. 12. At an absorbed pump power of 1.45 W, the pulse energy for Tm:YAP/WS_2 and Tm:YAP/MoS_2 lasers was 2.9 and 3.8 μJ, respectively. Similarly, with the increase of the absorbed pump power, the maximum peak powers of 1.23 and 1.55 W were obtained for the Tm:YAP/WS_2 and Tm:YAP/MoS_2 lasers.

The Q-switched properties of both Nd:YAP/WS_2 and Nd:YAP/MoS_2 lasers are summarized in Table 1. By comparison, MoS_2 with a modulation depth of 13.0% exhibited a higher capacity of energy storage than WS_2 with a modulation depth of 8.9%. The above experimental results have proven that WS_2 and MoS_2 can be promising saturable absorbers in the 2 μm laser range.

5. Conclusions

To the best of our knowledge, this is the first comparison of WS_2 and MoS_2 nanosheets serving as saturable absorbers in a passively Q-switched Tm:YAP laser. The 2D nanosheets of WS_2 and MoS_2 were prepared

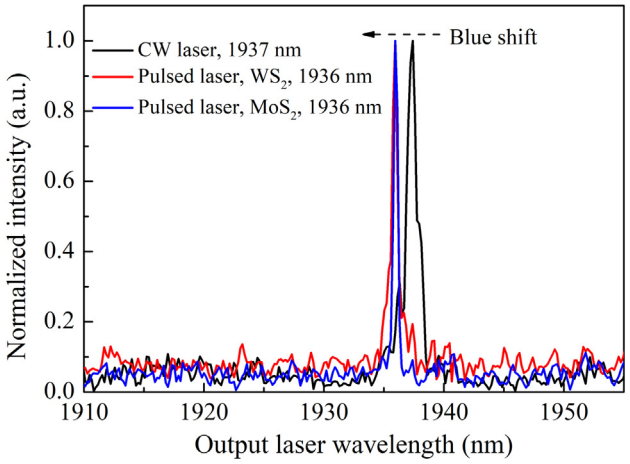

Fig. 10. The laser spectrum of CW and pulsed lasers.

by the CVD method. The microstructure and optical characteristics of the nanosheet were researched. The number of layers in the WS_2 and MoS_2 nanosheets were measured to be 4–5 and 3–4, respectively. The corresponding modulation depths were 8.96% and 13.0%, respectively. In Raman spectra, the characteristic peaks of A_{1g} and $E_{2g}{}^1$ appeared at 353.0 and 419.9 cm^{-1}, respectively, in the WS_2 nanosheet. For MoS_2, they occured at 384.9 and 408.8 cm^{-1}, respectively. The initial transmission of WS_2 and MoS_2 nanosheets was measured to be 85.5% and 84.7%, respectively, at 1937 nm. Subsequently, the CW and passively Q-switched Tm:YAP laser with WS_2/MoS_2 nanosheets at 2 μm were demonstrated. In the CW operation, the maximum output power of 2.8 W was obtained at an absorbed pump power of 6.9 W, when the radius of curvature of the output mirror was 50 mm. The corresponding slope efficiency was 46.4%. In a passively Q-switched operation, compared with the CW laser, the output spectral width was compressed and a blue shift occurred, which was caused by the shift of the resonator gain and loss at various wavelengths. At an absorber pump power of 1.45 W, the average output power, pulse width, repetition rate, pulse energy, and peak power for the Tm:YAP/WS_2 laser were 0.11 W, 2.65 μs, 34.7 kHz, 2.9 μJ, and 1.23 W, respectively. As for the Tm:YAP/MoS_2 laser, the average output power, pulse width, repetition rate, pulse energy, and peak power were 0.10 W, 2.50 μs, 24.0 kHz, 3.8 μJ, and 1.55 W, respectively.

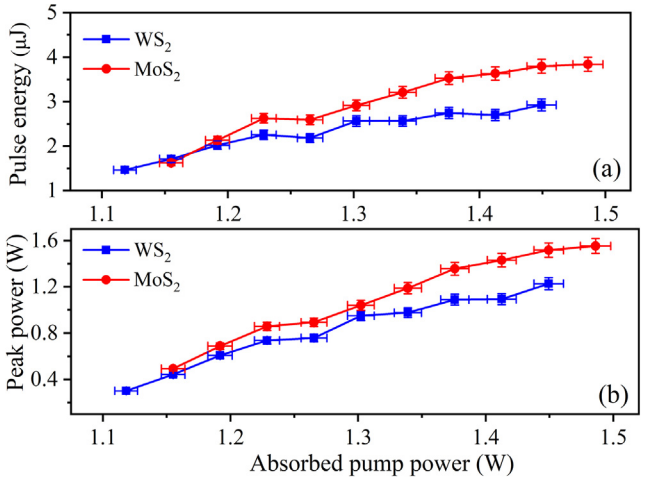

Fig. 12. The pulsed laser performance of the passively Q-switched Tm:YAP laser. (a) Pulse energy (b) Peak power.

CRediT authorship contribution statement

Yufei Ma: Conceptualization, Supervision. **Haiyue Sun:** Investigation, Writing - original draft. **Baofa Ran:** Data curation. **Shanchun Zhang:** Investigation. **Han Zhang:** Methodology. **Frank K. Tittel:** Writing - review & editing. **Zhiwei Lv:** Validation.

Declaration of Competing Interest

The authors declare that they have no known competing financial interests or personal relationships that could have appeared to influence the work reported in this paper.

Acknowledgement

This work was supported by the National Natural Science Foundation of China (Grant No. 61875047 and 61505041), the Natural Science Foundation of Heilongjiang Province of China (Grant No. YQ2019F006), Financial Grant from the Heilongjiang Province Postdoctoral Foundation (No. LBH-Q18052) and the Fundamental Research Funds for the Central Universities.

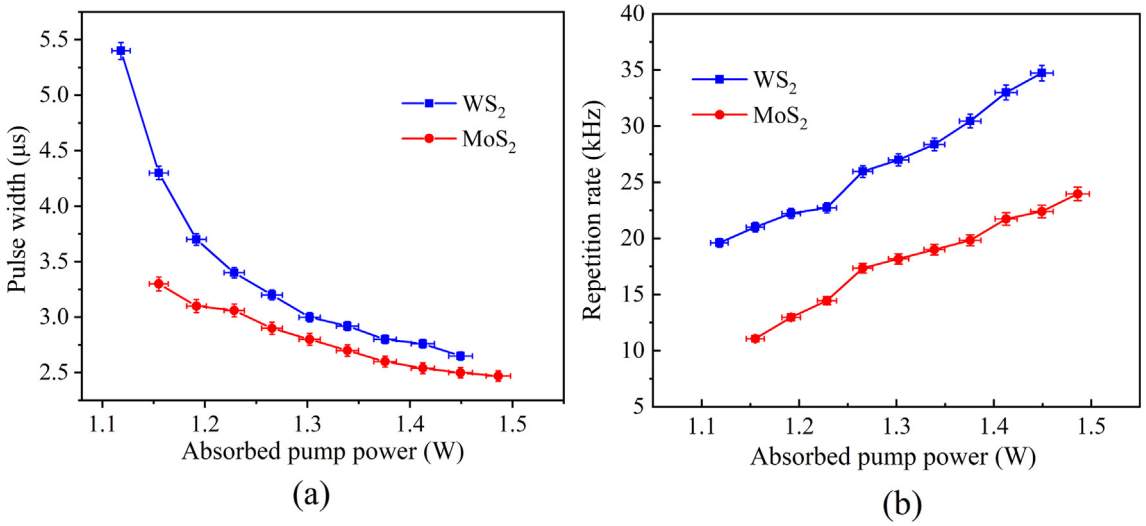

Fig. 11. The pulsed laser performance of the passively Q-switched Tm:YAP laser. (a) Pulsed width (b) Repetition rate.

Table 1
Comparison of passively Q-switched performance of Nd:YAP/WS_2 and Nd:YAP/MoS_2 lasers.

Laser	Maximum average output power (W)	Maximum repetition rate (kHz)	Narrowest pulse width (μs)	Maximum peak power (W)
Nd:YAP/WS_2	0.11 W	34.7	2.65	1.23
Nd:YAP/MoS_2	0.10 W	24.0	2.50	1.55

References

[1] I.F. Elder, J. Payne, Diode-pumped, room-temperature Tm:YAP laser, Appl. Opt. 36 (1997) 8606–8610.
[2] Y.F. Ma, Y. He, P. Patimisco, A. Sampaolo, S.D. Qiao, X. Yu, F.K. Tittel, V. Spagnolo, Ultra-high sensitive trace gas detection based on light-induced thermoelastic spectroscopy and a custom quartz tuning fork, Appl. Phys. Lett. 116 (2020) 011103.
[3] J. Liu, Y.G. Wang, Z.S. Qu, X.W. Fan, 2 μm passive Q-switched mode-locked Tm^{3+}: YAP laser with single-walled carbon nanotube absorber, Opt. Laser Technol. 44 (2012) 960–962.
[4] Y.F. Ma, H.J. Li, J.P. Lin, X. Yu, Greatly improved stability of passively Q-switched Ce:Nd:YAG laser by using corner cube prism, Laser Phys. 20 (2010) 1802–1805.
[5] T.L. Feng, S.Z. Zhao, K.J. Yang, G.Q. Li, D.C. Li, J. Zhao, W.C. Qiao, J. Hou, Y. Yang, J.L. He, L.H. Zheng, Q.G. Wang, X.D. Xu, L.B. Su, J. Xu, Diode-pumped continuous wave tunable and graphene Q-switched Tm: LSO lasers, Opt. Express 21 (2013) 24665–24673.
[6] N. Pavel, T. Dascalu, G. Salamu, O. Sandu, A. Leca, V. Lupei, Q-switched Nd lasers pumped directly into the $^4F_{3/2}$ emitting level, Opt. Commun. 282 (2009) 4749–4754.
[7] Y.F. Ma, X. Yu, X.D. Li, R.W. Fan, J.H. Yu, Comparison on performance of passively Q-switched laser properties of continuous-grown composite $GdVO_4$/Nd:$GdVO_4$ and YVO_4/Nd:YVO_4 crystals under direct pumping, Appl. Opt. 50 (2011) 3854–3859.
[8] P.G. Yan, A.J. Liu, Y.S. Chen, J.Z. Wang, S.C. Ruan, Passively mode-locked fiber laser by a cell-type WS_2 nanosheets saturable absorber, Sci. Rep. 5 (2015) 12587.
[9] C. Luan, K.J. Yang, J. Zhao, S.Z. Zhao, L. Song, T. Li, H.W. Chu, J.P. Qiao, C. Wang, Z. Li, S.Z. Jiang, B.Y. Man, L.H. Zheng, WS_2 as a saturable absorber for Q-switched 2 micron lasers, Opt. Lett. 41 (2016) 3783–3786.
[10] C. Wang, S.Z. Zhao, T. Li, K.J. Yang, C. Luan, X.D. Xu, J. Xu, Passively Q-switched Nd:LuAG laser using few-layered MoS_2 as saturable absorber, Opt. Commun. 406 (2018) 249–253.
[11] Y.F. Ma, Z.F. Peng, S.J. Ding, H.Y. Sun, F. Peng, Q.L. Zhang, Two-dimensional WS_2 nanosheet based passively Q-switched Nd:$GdLaNbO_4$ laser, Opt. Laser Technol. 115 (2019) 104–108.
[12] S. Manzeli, D. Ovchinnikov, D. Pasquier, O.V. Yazyev, A. Kis, 2D transition metal dichalcogenides, Nat. Rev. Mater. 2 (2017) 17033.
[13] L.J. Li, X.I. Yang, L. Zhou, W.Q. Xie, Y.L. Wang, Y.J. Shen, Y.Q. Yang, W.L. Yang, W. Wang, Z.W. Lv, X.M. Duan, M.H. Chen, Active/passive Q-switching operation of 2 μm Tm, Ho:YAP laser with an acousto-optical Q-switch/MoS_2 saturable absorber mirror, Photonics Res. 6 (2018) 614–619.
[14] Y.F. Ma, H.Y. Sun, Z.F. Peng, S.J. Ding, J.B. Peng, Q.L. Zhang, X. Yu, High efficiency diode-pumped continues-wave and passively Q-switched Nd:GSAG laser with a two-dimensional WS_2 saturable absorber at 1060 nm, Infrared Phys. Techn. 97 (2019) 371–375.
[15] M.W. Jung, J.S. Lee, J. Park, J. Koo, Y.M. Jhon, J.H. Lee, Mode-locked, 1.94-μm, all-fiberized laser using WS_2-based evanescent field interaction, Opt. Express 23 (2015) 19996–20006.
[16] K.F. Mak, C. Lee, J. Hone, J. Shan, T.F. Heinz, Atomically thin MoS_2: a new direct-gap semiconductor, Phys. Rev. Lett. 105 (2010) 136805.
[17] Q.H. Wang, K. Kalantar-Zadeh, A. Kis, J.N. Coleman, M.S. Strano, Electronics and optoelectronics of two-dimensional transition metal dichalcogenides, Nat. Nanotechnol. 7 (2012) 699.
[18] B. Peng, P.K. Ang, K.P. Loh, Two-dimensional dichalcogenides for light-harvesting applications, Nano Today 10 (2015) 128–137.
[19] A. Splendiani, L. Sun, Y.B. Zhang, T.S. Li, J. Kim, C.Y. Chim, G. Galli, F. Wang, Emerging photoluminescence in monolayer MoS_2, Nano Lett. 10 (4) (2010) 1271–1275.
[20] J.Y. Kim, S.M. Choi, W.S. Seo, W.S. Cho, Thermal and electronic properties of exfoliated metal chalcogenides, Bull. Korean Chem. Soc. 31 (2010) 3225–3227.
[21] H.K. Zhang, J.L. He, Z.W. Wang, J. Hou, B.T. Zhang, R.W. Zhao, K.Z. Han, K.J. Yang, H.K. Nie, X.L. Sun, Dual-wavelength, passively Q-switched Tm:YAP laser with black phosphorus saturable absorber, Opt. Mater. Express 6 (2016) 2328–2335.
[22] I.F. Elder, M.J.P. Payne, YAP versus YAG as a diode-pumped host for thulium, Opt. Commun. 148 (1998) 265–269.
[23] O.A. Buryy, D.Y. Sugak, S.B. Ubizskii, I.I. Izhnin, M.M. Vakiv, I.M. Solskii, The comparative analysis and optimization of the free-running Tm^{3+}:YAP and Tm^{3+}:YAG microlasers, Appl. Phys. B 88 (2007) 433.
[24] S.A. Payne, L.L. Chase, L.K. Smith, W.L. Kway, W.F. Krupke, Infrared cross-section measurements for crystals doped with Er^{3+}, Tm^{3+}, and Ho^{3+}, IEEE J. Quantum Electron. 28 (1992) 2619–2630.